17th World Conference on Earthquake Engineering, 17WCEE
Sendai, Japan - September 13th to 18th 2020

EXPERIMENTAL STUDY OF A RECYCLED PROTOTYPE OF A REAL SCALE FLUID VISCOUS DAMPER

Y. Taipicuri [1], C. Zavala [2], L. Nuñez [3]

[1] *Assistant Researcher, CISMID-Faculty of Civil Engineering - National University of Engineering, ytaipicurih@uni.pe*
[2] *Professor, CISMID-Faculty of Civil Engineering – National University of Engineering, czavala@uni.edu.pe*
[3] *Assistant Researcher, CISMID-Faculty of Civil Engineering - National University of Engineering, lnunezn@uni.pe*

Abstract

In Peru, severe past earthquakes have demonstrated that the majority of buildings did not collapse, but they would be severely damaged, as a consequence, their continuous functionality is affected, and the reparation cost is increased. Seismic protection systems are a good alternative to reduce structural damage by using various mechanisms such as seismic isolation or passive dampers. However, in Peru, there is a limited number of buildings with that kind of mechanism; nowadays, the seismic performance of new or retrofitted buildings with fluid viscous dampers is frequently analyzed through numerical simulations with data provided by the importing company of this device, indeed, there are not Peruvian fluid dampers. Furthermore, there is an informal market in Lima of pieces from disused or damaged construction machinery, which are sold like scrap metal. For these reasons, this research aims to develop at the structural laboratory of the Japan-Peru Center for Earthquake Engineering Research and Disaster Mitigation -CISMID a prototype of a fluid viscous damper to understand and estimate its dynamic behavior. To do so, a recycled hydraulic steel tube of a bulldozer was modified to manufacture the device in order to produce an environmentally friendly prototype with an acceptable behavior. Moreover, this prototype was manufactured by reducing complex processes of manufacturing to decree the construction costs because it has only an annular gap of 0. 5mm between the piston and the cylinder. A quasi-static cyclic loading test is performed to determine the properties of the prototype such as the hysteretic behavior, the effective damping ratio, and the damping coefficient of its linear behavior because the experiment is performed with low velocities. First, three specimens of two chambers were tested using glycerin as the hydraulic liquid; the piston was subjected to a sinusoidal displacement with an amplitude of ± 100 mm of stroke. Then, the prototype was modified to have one more chamber to contain nitrogen gas, also the hydraulic liquid was changed to silicon. Besides, the new amplitude of the sinusoidal displacement is ± 50 mm. Then, based on the data from the experiments, numerical models are proposed to describe the hysteretic behavior of the two types of prototypes. Finally, these prototypes are evaluated in a spring-mass model of one degree of freedom (SDOF) of a steel frame with these devices to perform a time history analysis to evaluate and compare the structural dynamic response.

Keywords: fluid damper, experimental test, full-scale specimen, recycled prototype

1. Introduction

There were carried out by SATREPS Project [1] several studies about a harmful scenario of a severe earthquake (Mw8.6-8.9) that will happen in Lima City [2]. In that sense, to reduce the vulnerability of structures around the world, a significant number of techniques and devices were developed. One of these devices is the fluid dampers, initially developed by the aerospace industry and then in the late eighties introduced in engineering applications [3]. Several studies were conducted to study the dynamic behavior of fluid dampers which fundamentally use silicon as a viscous liquid like the study carried out by C. Frings et al. [4] in 2017 about the development of a prototype of a viscous damper. Furthermore, in 2014, W. Pinaud [5] found in a reduced scale model (1:5) of a frame ensembled with a prototype, a similar behavior between the use of glycerin and silicon as a viscous liquid.

Moreover, in Lima City, the use of dampers is reduced to a limited number of structures [5] and these devices are imported. Additionally, there is an informal market of hydraulic bottles that belonged to disused machinery, now considered as scrap metal how is shown in Fig.1. For this reason, this investigation aims to develop and study a prototype of fluid damper with recycled materials available in the market. Hence, a hydraulic bottle was modified to build two hydraulic damper prototypes.

First, a specimen named TUNIZ was manufactured as described below; therefore, two prototypes of this specimen were tested by a quasi-static cyclic load performed by a static actuator due to the lack of equipment such as dynamic actuators in our university. The fluid force in this model is caused by the annular gap of 5mm which allows the pass of the glycerin between the two chambers; also, the stroke of this model was 100 mm. The hysteresis graph shows that the presence of air inside the specimen goes the cavitation phenomenon through the reduction of the viscous force. Then, to avoid cavitation phenomena, one prototype of the specimen TUNIZ was filled full of glycerin and, similarly, was tested; unfortunately, the seals and the bottle cap failed. However, this test was useful to measure the capacity of the bottle cap and the seals.

After that, a second specimen was manufactured based on a hydraulic monotube, and it was denominated TUNIZR2. For this purpose, the specimen of TUNIZ was modified to add a gas chamber, as is described below. Furthermore, the viscous fluid was changed to silicon. The hysteresis graph shows a combination between viscous resistant force, a friction component and a gas spring in order to adjust the hysteresis, the model proposed by G. Peckan [6] was used. Finally, a comparison between a SDOF model of a steel frame and other considering the use of a prototype of TUNIZR2 under a time history analysis of a Peruvian record getting as a result, a reduction of the response.

Fig. 1 – Pieces from disused or damaged construction machinery

2. Experimental program

2.1 Scheme of the prototype

The scheme of the two specimens developed is presented in Fig.2. The first specimen, named as TUNIZ, was based in the outline proposed by the study of W. Pinaud [5] of a reduced scale 1:5 prototype ensembled with a steel frame tested in a shaking table, the testing program considered was the use of many types of liquids; furthermore, that study indicates that glycerin and silicon gave better results. This prototype was scaled;

however, because one of the objectives of this investigation was to develop an environmentally friendly prototype considering the existence of an informal market of scrap metal in Lima, which is disused or damaged construction machinery, the authors decided to modify the measurement of the length of the piston and reduce the annular gap based on the work of C. Frings et al. [4]. Consequently, a recycled hydraulic steel tube of a bulldozer was modified, Fig.3 (a) shows the original components inside of the original steel tube. The construction procedure is listed as follows: First, the bottle and the piston road were trimmed as the dimensions required, as shown in Fig.3 (b). After, a steel cylinder was modified to be ensembled with the piston road in Fig.3 (c). Later, a screw cap of the cylinder was manufactured, inside that a symmetrical U-seal and an O-Ring were added to minimize costs, as is presented in Fig.3 (d). Afterward, the addition of the glycerin inside the bottle was manually performed, as is shown in Fig.3 (e). Finally, Fig.3 (f) shows the sealing of the bottle.

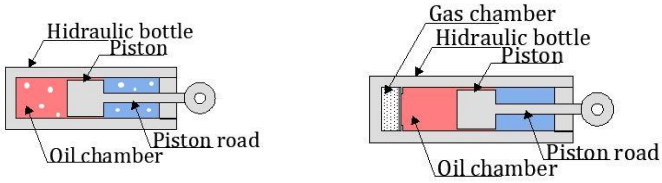

(a) TUNIZ (b) TUNIZR2

Fig. 2 – Scheme of the specimens

(a) Original components inside the hydraulic bottle

(b) Trimmed of the piston road

(c) Fabrication of the piston and ensembled

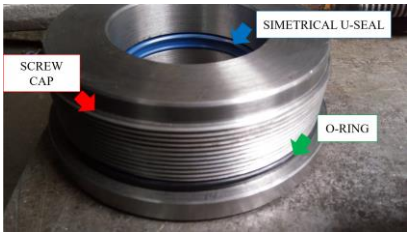

(d) Screw cap, inside the hydraulic U-seal and the O-ring

(e) Addition of glycerin in the bottle

(f) Manually sealing of the bottle

Fig. 3 – Construction procedure of TUNIZ

In order to improve the prototype, a second specimen was developed and was named as TUNIZR2. First, the hydraulic liquid was changed to silicon. Second, the outline was based on a hydraulic monotube; consequently, it was necessary to modify the initial prototype by creating a new chamber. Thereby, a gas regulator nipple of ¼ NPT was welded on the bottom of the bottle. Then, a new piston was manufactured, and three O-rings were ensembled with that. After that, an edge stop was welded to control the movement of the new piston, which separates the gas chamber and the fluid chamber. Finally, the gas chamber was filled with Nitrogen at 861.85 kPa of pressure, and this procedure is shown in Fig.4.

Fig. 4 – Construction procedure of TUNIZR2

2.2 Test specimens

The experimental program consisted of two types of specimens, two prototypes of the model TUNIZ, which was filled with glycerin, and one prototype of the model TUNIZR2. Also, both were tested on a quasi-static cyclic load test. The strokes considered of the specimens are 100 mm and 50 mm for TUNIZ and TUNIZR2, respectively. Furthermore, both models consider that the viscous force is going to be produced by the annular gap of 0.5 mm between the piston and the inner surface of the bottle along 200 mm in length of the piston. The measurement of both models is detailed in Fig.5. Moreover, Table 1 listed the components of the prototypes.

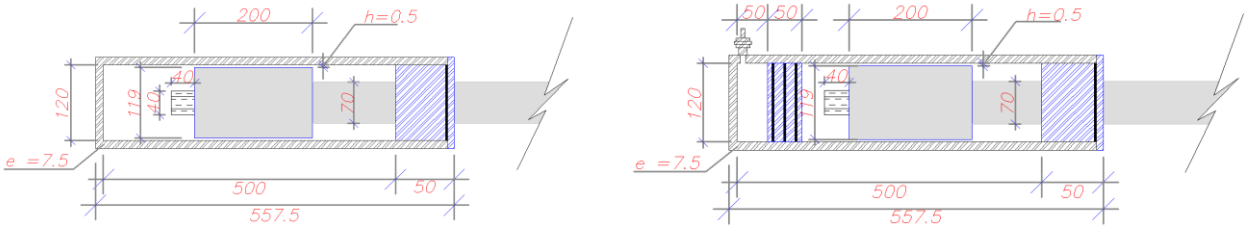

a) TUNIZ b) TUNIZR2

Fig. 5 – Measure of the prototypes in millimeters

Table 1 – List of elements of the prototypes

Components	**Model**
Hydraulic bottle: *Seamless cold-drawn steel tube*	TUNIZ, TUNIZR2
Piston road: *steel chrome bar*	TUNIZ, TUNIZR2
Piston, nut and screw cap: *steel*	TUNIZ, TUNIZR2
Glycerin USP	TUNIZ
1 U-seal and 1 O-ring on the screw cap	TUNIZ, TUNIZR2
Edge stop, chamber separator piston: *steel*	TUNIZR2
3 O-rings of the separator piston	TUNIZR2
Silicon 1000 cSt	TUNIZR2
Gas regulator nipple of ¼ NPT	TUNIZR2

2.3 Test setup

The test setup of the experiment and loading system consists of a steel frame connected to a strong floor. At the top, a hydraulic jack was assembled and was fixed in the beam by twelve high strength threaded bolts. Furthermore, the top of the specimen is fixed to the actuator by four high strength threaded bolts, and steel rollers control the control of displacement on sides. At the bottom of the prototype, the steel plate was joined to a steel stand using four high strength threaded bolts. Similarly, this support was attached to a strong floor. The hydraulic jack is a static actuator that is manually controlled in order to reproduce the desired test by a required displacement control of a maximum stroke of 200 mm and a maximum force of 498 kN. A pressure of 150 psi was used during the testing procedure. The following Fig.6 shows the test setup.

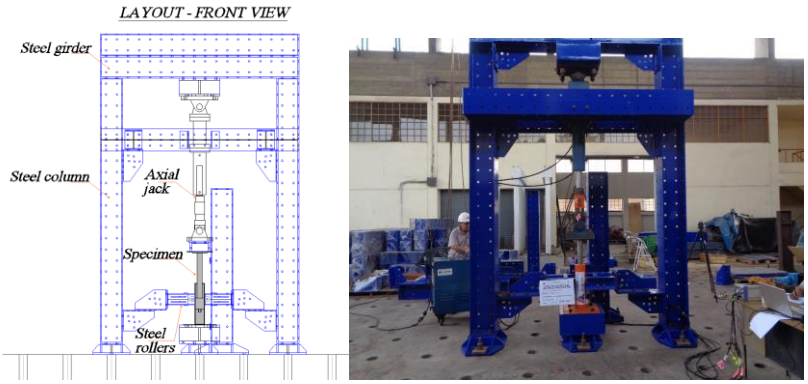

Fig. 6 – Experimental setup

2.4 Instrumentation

For the measurement of the response of the prototype, four linear voltage displacement transducers (LVDTs) were used; the detail of the instrumentation layout is displayed in Fig.7, where two of them have a range of 200 mm and measured the displacement of the piston road. The other two were used to control the displacement off-load application axis. Moreover, Table 2 listed the range of each LVDT.

a) b) c)

Fig. 7 – Layout of the placement of LVDTs

Table 2 – List of the range of the LVDTs

Label of channel	Length of run (mm)	Label of channel	Length of run (mm)
CH - 01	±200	CH - 03	±50
CH - 02	±200	CH - 04	±30

2.5 Testing procedure

The experiment procedure consists of the application of three amplitude objectives. For the first specimens, the amplitude was fixed in ten cycles of 33 mm, five cycles of 67 mm and five cycles of 95 mm. For the second model, there were planned to put nineteen cycles of 20 mm, eleven cycles of 35 mm, and three cycles of 50 mm; however, the last amplitude could not be tested because there was a failure in the gas nipple.

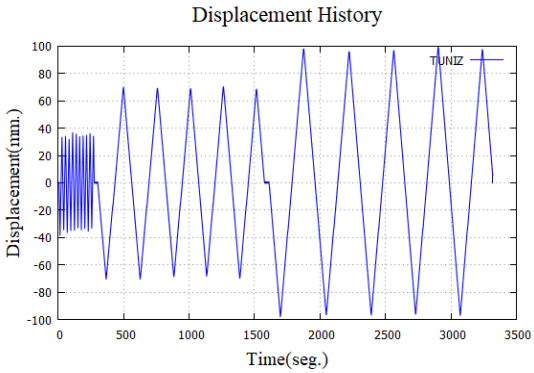

Fig. 8 – History of displacements of TUNIZ

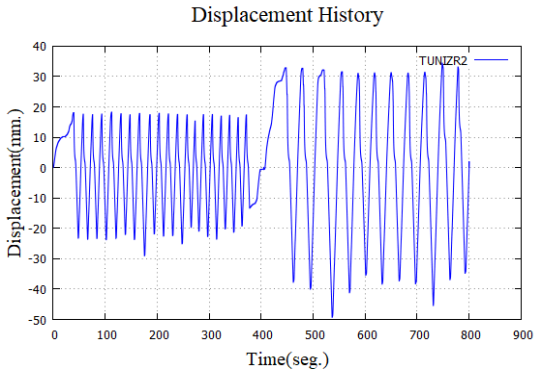

Fig. 9 – History of displacements of TUNIZR2

3. Results and Discussion

3.1 General observation of the specimens

For the prototypes of TUNIZ specimen, there were not found damage in the prototypes, loss of liquid or deformation in the areas near the strength threaded bolts, as is shown in Fig.10 (a). Although, because during the construction process there were not fully filled with glycerin, cavitation phenomena was observed in the hysteresis graph (see Fig.12) by the loss of force and affecting to develop an ellipsoidal loop.

For the prototype of the modified TUNIZ specimen, which was full filled with silicone, there were observed that after a displacement of 28.175mm with a resistant force of 164 kN a failure in the threaded bottle cap was observed as is shown in Fig.10 (b). The failure mechanism was, first, in the screw cap and the O-ring then followed by the liquid leak caused by the internal pressure. After that, this specimen could not be reused because the cap failure prevents the opening of the bottle.

For the prototype of the TUNIZR2 specimen, the failure was observed in the second amplitude of testing, and it was caused because the capacity of the gas regulator nipple was not enough for the pressure produced by the compression of the gas. Consequently, the gas escaped from the chamber then the liquid leak through the nipple (see Fig.10 (c)).

a) b) c)

Fig. 10 – Final state after testing a) TUNIZ, b) TUNIZ full filled, c) TUNIZR2

3.2 Hysteretic behavior

3.2.1 Hysteresis models

In order to fit the experimental data of TUNIZ, the hydraulic damper model [7] with linear characteristics was adopted due to the low values of velocities applied by the static actuators. Then, the behavior is given by the Eq. (1). In which F_{vd} is the damping force, V is the velocity of the prototype, and C_H is the damping coefficient.

$$F_{vd} = C_H V \tag{1}$$

Based on Eq. (1), the hysteresis model of TUNIZ prototypes is dependent on the parameter C_H. A model proposed by Peckan [6] was adopted to fit the hysteresis curve of TUNIZR2. This model proposes that the resultant force is produced by a component dependent on the velocity dependence (viscous force) and a spring component; this relationship is shown in Eq. (2).

$$F_t = F_v + F_s \tag{2}$$

Where F_t is the total force, F_v is the viscous force, and F_s is the spring force, which is a combination between the friction force of the piston and the gas spring. The viscous component proposed in this model is represented by an expression which includes the nonlinear behavior by the viscous rate, and also consider the characteristics of a self-returning damper as follows:

$$F_v = C\ sign(\dot{x})\ |\ \dot{x}\ |^{\alpha}\ |x/x_{max}|^{\beta} \tag{3}$$

In which $\dot{x}$ is the velocity of the prototype, x_{max} is the maximum value of the stroke, C is the damper constant, α and β are the velocity exponent and the mechanical configuration exponent respectively. The spring force is represented by a bilinear model to define the skeleton curve, which is shown as follows. This model was proposed first by Menegotto and Pinto (1973) [8].

$$F_s = K_2\ x + ((K_1 - K_2)\ x)/\ (1+|\ (K_1\ x)\ /\ P_y\ |^{R})^{1/R} \tag{4}$$

Where x is the stroke of the prototype, K_1 is the initial stiffness, K_2 is the elastomeric stiffness, P_y is the limit force until the nonlinear behavior, and R is the shape factor. As is shown in Fig 2, the second prototype has an asymmetric distribution; for this reason, the equation proposed by Peckan is modified, so the following equations are proposed to describe the hysteretic behavior.

$$x>0: \qquad F_t = K_2\ x + ((K_1 - K_2)\ x)/\ (1+|\ (K_1\ x)\ /\ P_y\ |^{R})^{1/R} + C\ sign(\dot{x})\ |\ \dot{x}\ |^{\alpha}\ |x/x_{max}|^{\beta} \tag{5}$$

$$x<0: \qquad F_t = K_4\ x + ((K_3 - K_4)\ x)/\ (1+|\ (K_3\ x)\ /\ P_{y2}\ |^{R})^{1/R} + C\ sign(\dot{x})\ |\ \dot{x}\ |^{\alpha}\ |x/x_{max}|^{\beta} \tag{6}$$

Where Eq. (5) describe the behavior when the jack is pushing the ensembled system of the piston road, the piston to the bottom and, consequently compressing the gas chamber; moreover, the displacement in this direction was considered positive. On the other hand, when the jack is pulling Eq. (6) describe its behavior, both behaviors are illustrated in Fig.11. Based in those equations, the hysteresis model of the second prototype is dependent of the following parameters: K_2, K_1, K_3, K_4, P_y, P_{y2}, R, C, α, β.

As is described before, in this case, the velocity was not measured, even though it was calculated by the central differential method.

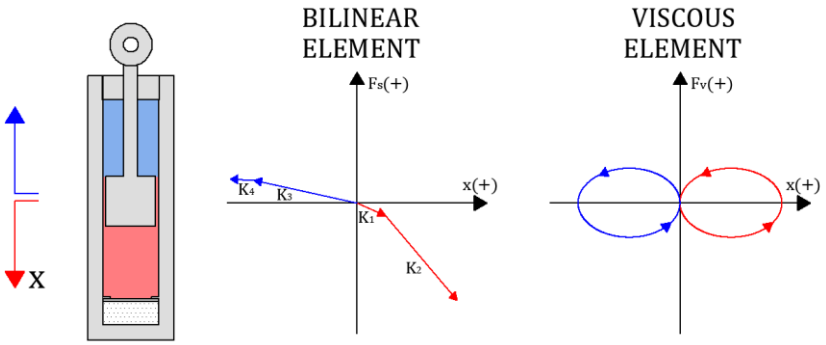

Fig. 11 – Components of the total force from Peckan hysteresis model

3.2.2 Modified Firefly Algorithm

To fit the hysteresis curve with the experimental curves, the modified firefly algorithm proposed by Zaman M. [9,10] was used by employing the Peckan model and hydraulic damper model. For TUNIZ specimens, in order to describe the experimental behavior based on Eq. (1), the parameter C_H was calculated by the comparison of the dissipated energy of each loop. There were calculated two values of C_H, one for the first amplitude and the other for the second and third amplitude of testing. The number of parameters used for the algorithm was 1000 fireflies for 200 generations. The comparison is illustrated in Fig 12, and the values of the parameter are described in Table 3. As is shown in Fig 12, the linear model does not describe the behavior of the prototypes caused by the cavitation phenomena; for this reason, the authors considered to develop TUNIZR2.

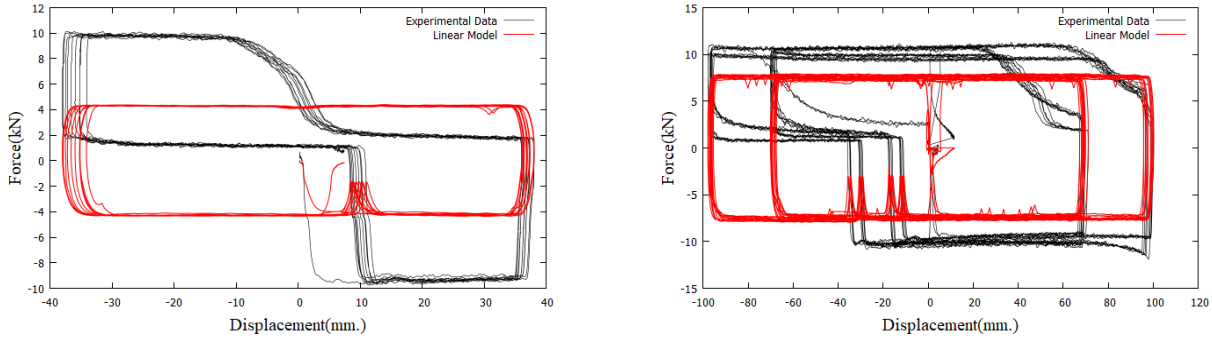

a) b)

Fig. 12 – Hysteresis curve of the first type of specimen a) TUNIZ-1, b) TUNIZ-2

Table 3 – Curve Fit Parameters of TUNIZ

Parameter	**TUNIZ (33mm) *kN*s/mm***	**TUNIZ (67 – 95 mm) *kN*s/mm***
C_H	-0.753	-1.297

For the TUNIZR2 specimen, there were carried out 1000 generations with 500 fireflies in each one. There were taken into consideration ten parameters; consequently, the dimension of the solution space was 10. The comparison between the experimental data and the hysteresis model is presented in Fig.13 furthermore, as is mentioned before, in Fig.13. (b) is possible to appreciate the failure located in the gas chamber by the loss of strength, as is shown in the two last loops. With this model, the numerical data is getting a better approach to the experimental data compared with the first specimen.

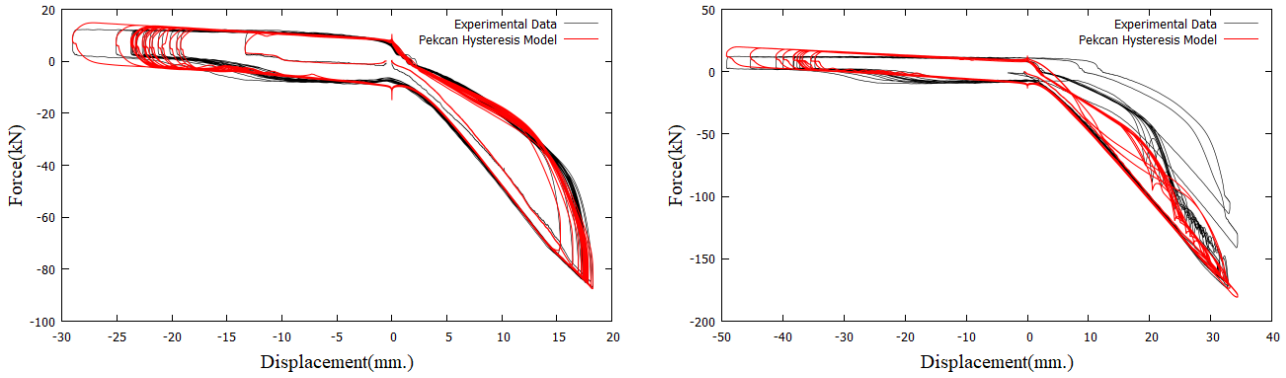

Fig. 13 – Hysteresis curve of the TUNIZR2 prototype a) TUNIZR2-1with an amplitude of 20 mm., b) TUNIZR2-1 with an amplitude of 35 mm

Table 4 – Curve Fit Parameters of TUNIZR2

K_1 (kN/mm)	K_2 (kN/mm)	P_y (kN)	K_3 (kN/mm)	K_4 (kN/mm)	P_{y2} (kN)	R	C (kN*s/mm)	α	β
-0.210	-0.257	-0.657	-0.692	-5.713	2.414	1.730	-0.928	1.225	-0.051

3.3 Energy dissipation capacity

The value of the energy dissipation for each cycle was computed from the enclosed area of the hysteresis loops. The average dissipated energy is shown in Table 5. Furthermore, the damping factor (h) was calculated from the specimens, as shown in Eq. (7) [11]. Where ΔW is the work done by the damping force in one cycle named dissipated energy, and W is the maximum potential energy. Fig.14 is presented the equivalent viscous damping of the specimens.

$$h = \frac{1}{4\pi}\frac{\Delta W}{W} \tag{7}$$

Table 5 – Average energy dissipation at different drift ratios

	TUNIZ-01			**TUNIZ-02**			**TUNIZR2-01**	
Amplitude	33 mm	65 mm	95 mm	33 mm	65 mm	95 mm	20 mm	35 mm
Average energy dissipated per cycle (kN.mm)	57.997	204.203	321.077	60.853	187.900	300.318	736.004	1578.374

From Table 5 is possible to see that TUNIZR2 dissipates more energy than TUNIZ per each cycle and with less amplitude. Moreover, TUNIZR2 specimen has a higher equivalent viscous damping than the TUNIZ specimen, which indicates that with lower displacement, it is possible to have a higher rate of equivalent viscous damping as is shown in Fig.14.

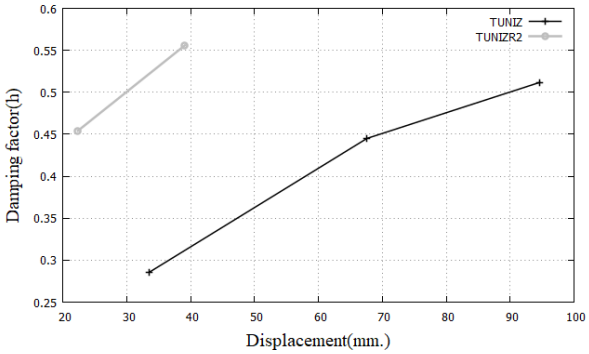

Fig. 14 – Equivalent viscous damping ratio

3.4 Numerical simulation analysis

In this section, a mathematical model of a steel frame is considered as an SDOF model and is represented by a bilinear spring, as is shown in Fig.15. A pushover analysis was performed, then the following properties were determined: the initial stiffness of this spring is 10.99 kN/mm, the post-yielding stiffness is 2.22 kN/mm, the yielding displacement is 46.67mm, the weight is considered as 205.40 kN, and the inherent damping is considered as 0.05. Then, the steel frame with the TUNIZR2 was modeled considering the parameters of the Peckan model. The value of peak ground acceleration (PGA) was defined as 0.45g according to the E030 Peruvian Standard [12] considered for a common building located in Lima with a hard soil site; moreover, the selected record to be used was Lima earthquake (17/10/1966) N-S direction as shown in Fig.16.Subsequently, a nonlinear time history analysis was performed using the explicit Newmark integration method to solve the equation of motion. After that, time history analysis was performed; the results show that the response displacement was reduced, as shown in Fig.17, and the hysteresis response of the system is illustrated in Fig.18. Further, it is important to mention that this analysis is an idealization of the predicted behavior of TUNIZR2 because the velocities reached in this analysis are higher than in the test.

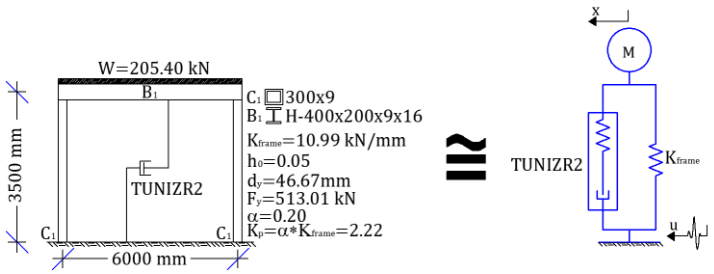

Fig. 15 – Steel frame to be analyzed and mathematical single degree of freedom model (SDOF)

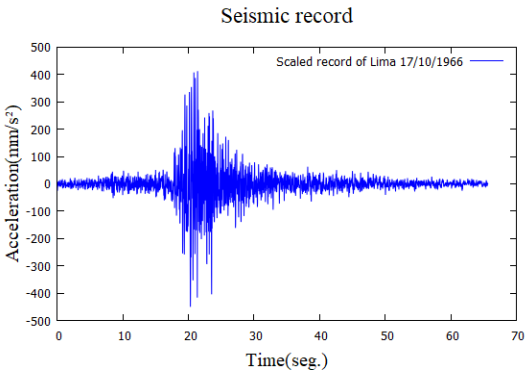

Fig. 16 – Accelerogram of the scaled record of Lima earthquake (1966) N-S component

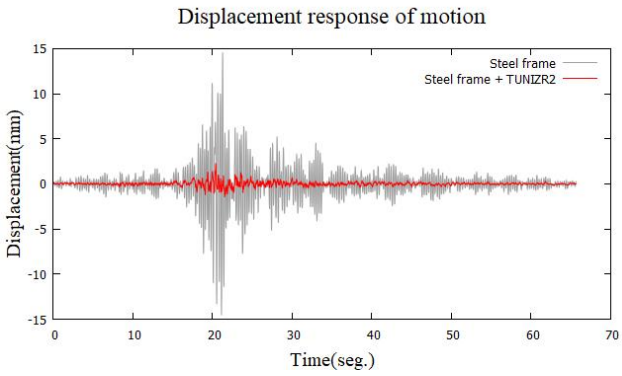

Fig. 17 – Comparison of the displacement response

It can be seen from Fig.17 that the displacement response is reduced by adding the prototype around five times. Also, the comparison between the hysteresis of both systems remains linear, as is shown in Fig.18. Furthermore, Fig.19 shows the hysteretic behavior of the TUNIZR2 prototype of the behavior of the composed system with the predicted values. Also, this graph shows that the viscous resistant force is higher than the spring force caused by the low values of displacement.

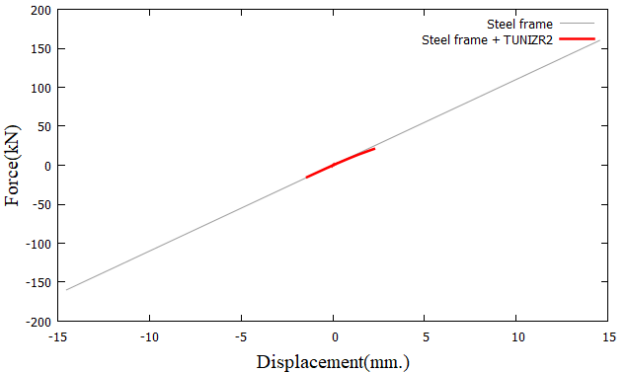

Fig. 18 – Force-displacement graph of response of SDOF model when subjected to the scaled record of Lima earthquake (1966)

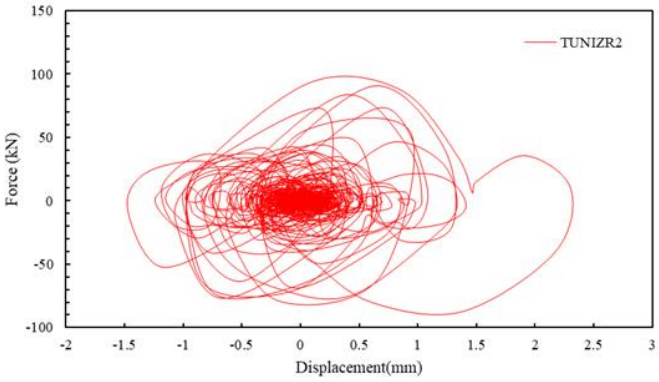

Fig. 19 – Force-displacement graph of the response of TUNIZR2

5. Conclusion

In this paper, the authors describe the constructive procedure to develop the prototypes from scrap metal, the result of a quasi-static cyclic load test, and the seismic response of a nonlinear time history analysis of an SDOF. The findings of this study are as follows:

- It is possible to reused materials to manufacture a damper device with an annular fluid-resistant force.
- From the quasi-static cyclic load test, this investigation presents a previous step for the development of a viable product; however, a dynamic cyclic loading test is necessary to measure the relationship between high velocities and resistance forces. In this study, the velocities measured on the experiments were low values with a maximum of 18.767 mm/s.
- From the results of TUNIZ, the cavitation phenomena affect the hysteresis loop by losing the viscous force; consequently, less energy is being dissipated. Moreover, the mathematical model fits with the experimental data based on the equivalence of dissipated energy.
- From the results of TUNIZR2, an asymmetric device was tested, in one direction the viscous force was predominant. On the other hand, in the other direction a combination of a significant gas spring and friction force caused by the separator piston, gas chamber and the viscous force reached a maximum force of 173.553kN for a displacement of 33 mm. The experimental curve was fitted with the hysteresis model proposed by Peckan with good accuracy. However, the specimen failed because the low capacity of the gas nipple, for this reason, is recommended for future works to use a nipple with a higher pressure capacity and the developing of a specimen with four-chamber (two as gas chamber) in order to have a symmetrical response in combination of viscous force, frictional force, and gas spring. Furthermore, it is suggested that the hydraulic seals of the bottle cap will be improved for higher pressure. The energy dissipation of TUNIZR2 shows to be higher than TUNIZ, with higher damping factors correlated to fewer displacements.
- From the nonlinear time history analysis, a reduction in the displacement response of the building with the TUNIZR2 prototype in around five times. Moreover, the predominant component was the viscous force how is shown in Fig. 19 caused the less value of the movement.

6. Acknowledgements

The authors want to express their gratitude to the Vice-Rectorate of the National University of Engineering (Peru) for its support to the developing of this research. Also, the authors would like to thank to the Structural Laboratory of Peruvian Japanese Center of Seismic Research and Disaster Mitigation (CISMID). Besides, a special thanks to Professor C. Zavala for his guidance and gratitude to Professor Roy Reyna, Andre Muñoz and Larry Cardenas.

7. References

[1] Yamazaki F., Zavala C., Nakai S., Koshimura S., Saito T. and Midorikawa S. (2010): *Enhancement of earthquake and tsunami disaster mitigation technology in Peru: A SATREPS project.*

[2] Pulido N., Tavera H., Perfettini H., Chlieh M., Aquilar Z., Aoi S., Nakai S. and Yamazaki F. (2011): Estimation of Slip Scenarios for Megathrust Earthquakes: A case study for Peru, *The 4th IASPEI/IAEE International Symposium*, Santa Barbara.

[3] Taylor D.P. (1996): Fluid dampers for applications of seismic energy dissipation and seismic isolation. *11th World Conference on Earthquake Engineering*, Acapulco, Mexico.

[4] Frings C., Zemp R., De La Llera J.C. (2017): Multiphysics modeling, experimental validation and building implementation of viscous fluid dampers. *16th World Conference on Earthquake Engineering*, Santiago de Chile, Chile.

[5] Pinaud. W.Y., (2014): Estudio experimental de las características dinámicas de un dispositivo disipador viscoso a escala reducida. Undergraduate Thesis. National University of Engineering, Peru.

[6] Pekcan G., Mander J., M. EERI, and Chen S. (1995): The Seismic Response of a 1:3 Scale Model R.C. Structure with Elastomeric Spring Dampers, *Earthquake Spectra*, **11°**(2), 249-267.

[7] Higashino M., Okamoto S. (2006): *Response Control and Seismic Isolation of Buildings*. Taylor & Francis: London, 1st edition.

[8] Menegotto M.; Pinto P. E. (1973): Method of Analysis for Cyclically Loaded R.C. Plane Frames Including Changes in Geometry and Non-Elastic Behavior of Elements under Combined Normal Force and Bending, *IABSE Symposium on the Resistance and Ultimate Deformability of Structures Acted on by Well Defined Repeated Loads*, Preliminary Report pp. 15-22, Lisbon, Portugal.

[9] Zaman M.A., Sikder U. (2015): Bouc–Wen hysteresis model identification using Modified Firefly Algorithm. *Journal of Magnetism and Magnetic Materials*, **395°**, 229-233.

[10] A. Muñoz, M. Diaz, y R. Reyna (2019): Applicability study of a low-cost seismic isolator prototype using recycled rubber, *Tecnia*, **29°**(2), 65-73.

[11] Shibata A (2010): Dynamic Analysis of Earthquake Resistant Structures. Tohoku University Press, 2 nd edition.

[12] SENCICO (2018): Standard E.030 Seismic Design. National Building Regulations, Lima, Peru. (In Spanish).

